

Formation of Highly Efficient, Long-Lived Charge Separated States in Star-Shaped Ferrocene-Diketopyrrolopyrrole-Triphenylamine Donor-Acceptor-Donor Conjugates

Charu Popli,^{[a]‡} Youngwoo Jang,^{[b]‡} Yuvraj Patil,^[a] Rajneesh Misra^{[a]*} and Francis D'Souza^{[b]*}

Abstract: The significance of multiple number of donor-acceptor entities on a central electron donor in a star-shaped molecular system in improving light energy harvesting ability is reported. For this, donor-acceptor-donor type conjugates comprised up to three entities ferrocenyl (Fc)-diketopyrrolopyrrole (DPP) onto a central triphenylamine (TPA), (**4-6**) by the Pd-catalyzed Sonogashira cross-coupling reactions have been newly synthesized and characterized. Donor-acceptor conjugates possessing diketopyrrolopyrrole (1 to 3 entities) onto the central triphenylamine, (**1-3**) served as reference dyads while monomeric DPP and Fc-DPP served as control compounds. Both DPP and Fc-DPP carrying conjugates exhibited red-shifted absorption compared to their respective control compounds revealing existence of ground state interactions. Furthermore, DPP fluorescence in **4-6** was found to be quantitatively quenched while for **1-3**, this property varied between 73-65% suggesting occurrence moderate amounts of excited state events. The electrochemical investigations exhibited an additional low potential oxidation in the case of Fc-DPP-TPA based derivatives (**4-**

6) owing to the presence of ferrocene unit(s). This was in addition to DPP and TPA redox peaks. Using spectral, electrochemical and computational studies, Gibbs free-energy calculations were performed to visualize excited state charge separation (ΔG_{CS}) in these donor-acceptor conjugates as a function of different number of Fc-DPP entities. Formation of Fc^+-DPP^--TPA charge separated states (CSS) in the case of **4-6** was evident. Using spectroelectrochemical studies, spectrum of CSS was deduced. Finally, femtosecond transient absorption spectral studies were performed to gather information on excited state charge separation. Increasing the number of Fc-DPP entities in **4-6** improved charge separation rates. Surprisingly, lifetime of the charge separated state, Fc^+-DPP^--TPA was found to persist longer with an increase in the number of Fc-DPP entities in **4-6** as compared to Fc-DPP-control and simple DPP derived donor-acceptor conjugates in literature. This unprecedented result has been attributed to subtle changes in ΔG_{CS} and ΔG_{CR} and the associated electron coupling between different entities.

In recent years, the field of organic electronics has drawn great deal of attention of scientific community.^[1,2] In this regard, organic small molecule derived donor-acceptor (D-A) frameworks with extensive π -conjugation have been studied for their wide range of optoelectronic applications including photovoltaics,^[3] nonlinear optical (NLO) switches, sensors, fluorescent near-infrared (NIR) probes, and data storage devices.^[4,5] Further, the optoelectronic properties of D- π -A type framework can be geared towards better performance by designing D- π -A- π -D or A- π -D- π -A, type multi-molecular systems.^[6,7] Although a number of D- π -A type simple systems have been synthesized and studied in literature, multi-modular systems π -connected to higher numbers donor and acceptors revealing better performance of light induced events have been scarce due to synthetic and property evaluation challenges.

Diketopyrrolopyrrole (DPP) is a π -conjugated bicyclic di-lactam moiety and is one of the widely used organic dyes due to its relatively simple synthesis.^[8,9] DPP derivatives exhibit poor solubility in organic solvents due to strong π - π and H-bonding

interactions but the *N*-alkylation enhances their solubility in common organic solvents.^[10,11] DPPs possess features like relatively strong electron accepting property, excellent thermal stability, macrocycle rigid-planarity and high fluorescence quantum yields.^[12,13] Further, covalently linked thiophene-DPP (*i.e.*, dithienyl DPP) led to small organic molecules extending their absorption well into the visible region. A literature survey reveals that DPP coupled with a variety of donors have been explored as small organic molecule based bulk heterojunction (BHJ) solar cell applications.^[12-15] Among the various donors, ferrocene is one of the widely used donors due to its excellent thermal and photochemical stability as well as strong NLO response.^[15a-b] Ferrocene also undergoes facile oxidation, consequently, it has been widely used in building donor-acceptor systems for charge separation and stabilization.^[15c-k]

A variety of linear and star-shaped DPP derived donor-acceptor systems have been reported for optoelectronic applications.^[14] For example, a series of star-shaped molecules with fused aromatic ring 1,3,5-tri(thiophen-2-yl) benzene (TTB), 2,4,6-tri(thiophen-2-yl)-1,3,5-triazine (TTT) as core for organic semiconductors have been reported.^[16] Triphenylamine (TPA) is widely used as an electron donor in the design of efficient D-A based molecules. Many star-shaped small molecules based on TPA as a central core have been widely studied for organic photovoltaics.^[17] The special propeller structure of TPA is known to form amorphous materials promoting close contact with the acceptors leading to poor phase separation and charge recombination, leading to enhanced charge dissociation efficiency.^[18-19]

In the present investigation, we have re-designed our approach of constructing multi-modular donor-acceptor systems

[a] Department of Chemistry, Indian Institute of Technology, Indore 453552, India. E-mail: rajneeshmisra@iiti.ac.in

[b] Department of Chemistry, University of North Texas, 1155 Union Circle, #305070, Denton, TX 76203-5017, USA, E-mail: Francis.DSouza@UNT.edu

‡ Equal contribution

□ Supporting information for this article, Synthetic, spectral, ¹H and ¹³C NMR, MALDI-mass, additional fs-TA spectral, and computational results.

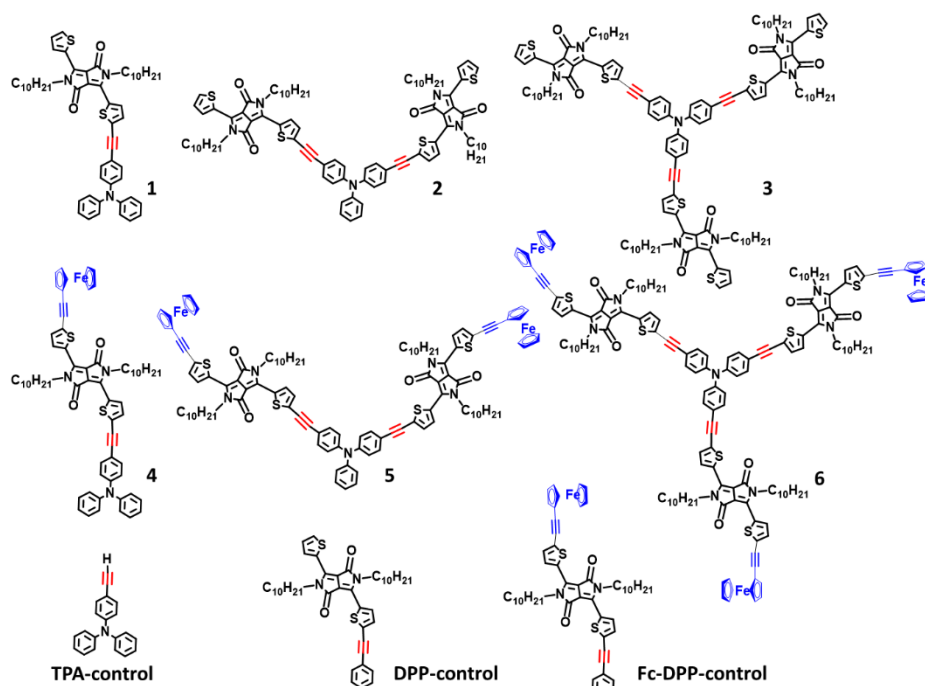
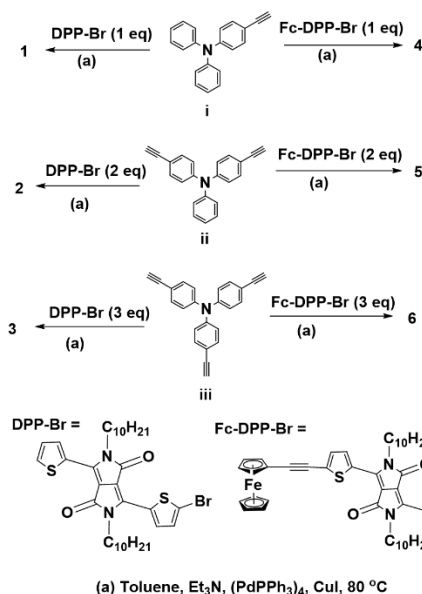


Figure 1. Chemical structures of the investigated DPP and ferrocenyl-DPP functionalized TPA compounds, **1–6** along with the control compounds.



Scheme 1. Synthesis of DPP and ferrocenyl-DPP functionalized TPA compounds, **1–6**. For complete structures of **1–6** see Figure 1.

wherein the central TPA is functionalized to carry 1 to 3 entities of electron acceptor dithienyl-DPP entities (compounds **1–3** in Figure 1). Further, a much stronger electron donor ferrocene is introduced onto the opposite side of dithienyl-DPP entity (compounds **4–6** in Figure 1) to modulate the electrochemical and photochemical properties. We demonstrate here that introduction of ferrocene alters the photochemistry leading to efficient formation of Fc⁺-DPP⁻-TPA CSS in the case of compounds **4–6** instead of relatively inefficient DPP⁻-TPA⁺ CSS observed in the case of compounds **1–3**. Further, improved persistence of CSS upon increasing the Fc-DPP entities, that is, long-lived CSS due

to varied degree of electron coupling, is demonstrated using transient spectroscopic technique. It may be mentioned here that long-lived charge separated states in donor-acceptor systems is one of the key determinants for the photovoltaic performance of dye-sensitized solar cell and photocatalytic applications.^[19c-d]

The mono-, di- and tri- DPP substituted TPA (**1–3**) were synthesized by the palladium catalyzed Sonogashira cross-coupling reaction of compounds i, ii and iii with 1.0, 2.0 and 3.0 equivalents of monobromo DPP (DPP-Br) in 75%, 60% and 65% yields, respectively (Scheme 1). Recently we have reported the synthesis of **1** and we have taken it here for the sake of comparison.^[7d] The mono-, di- and tri- ferrocenyl-DPP based derivatives with TPA as central core (**4–6**) were synthesized by palladium catalyzed Sonogashira

cross-coupling reactions of compounds i, ii and iii with 1.0, 2.0 and 3.0 equivalents of mono bromo ferrocenyl-DPP in 60%, 62% and 65% yields, respectively (Scheme 1). The newly synthesized compounds were purified by repeated silica gel column chromatography and recrystallization techniques. All these compounds were readily soluble in common organic solvents and were fully characterized by common spectroscopic techniques (¹H NMR, ¹³C NMR, HRMS and MALDI, see SI for additional synthetic and spectral details).

Table 1. Optical absorption and emission peak maxima, fluorescence lifetime, charge separation rate, and first reduction and first oxidation potential of the investigated compounds in DCB.

Compound	λ_{Abs} , nm	λ_{Em} , nm	τ_{Fl} , ns	k_{CS} , s ⁻¹	Potential V vs. Ag/AgCl	
					E_{red}	E_{ox}
DPP-control	545 586	612	3.98	--	-1.04	1.03
Fc-DPP control	582 628	--	--	--	-0.98	0.74
1	559 594	628 672	2.48	1.52×10^8	-1.02	1.00
2	559 594	627 672	2.31	1.82×10^8	-0.97	1.02
3	562 600	631 675	1.90	2.75×10^8	-0.92	1.07
4	592 636	-- --	--	--	-0.99	0.76
5	592 636	-- --	--	--	-0.95	0.74
6	592 636	-- --	--	--	-0.91	0.73

Figure 2a shows solution color of compounds **1–6** in series. Compounds **1–3** revealed magenta-red color while **4–6** revealed cyanine-blue, suggesting different degrees of ground state interactions in these two series of compounds. This is further confirmed by absorption spectra of **1–6** along with control compounds shown in Figure 2b while the optical data are summarized in Table 1. DPP-control revealed peaks at 545 and 586 nm, and these peaks were red-shifted by up to 18 nm in the

COMMUNICATION

case of **1-3**. The red-shift gradually increased with an increase in the number of dithienyl-DPP entities on TPA. Appending a ferrocenyl entity on DPP in Fc-DPP-control caused additional red-shift with peak maxima to 582 and 628 nm. In the case of **4-6**, these two peaks were further red-shifted by ~8 nm indicating different degrees of interactions between dithienyl-DPP entities with central TPA and terminal ferrocene entities.

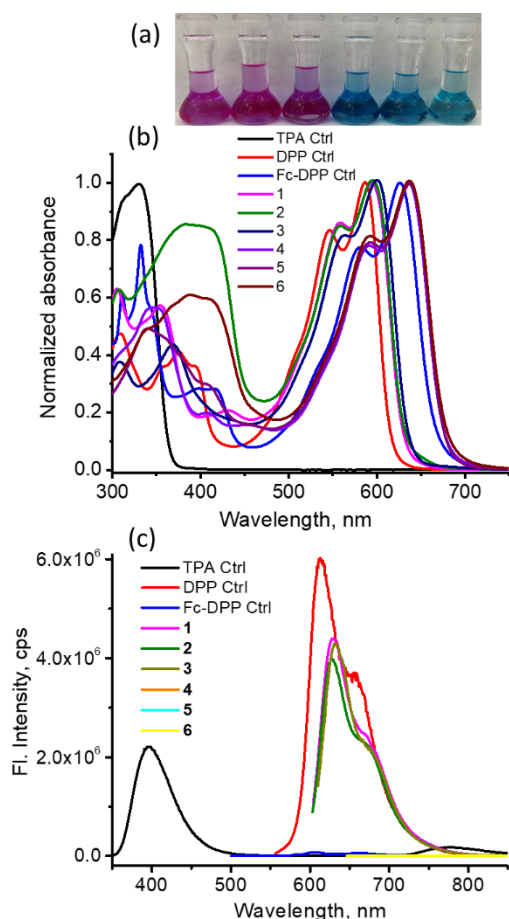


Figure 2. (a) Picture of solution color of compounds **1-6** in series at ambient light, (b) normalized absorption and (c) fluorescence spectra of the investigated compounds in DCB. The compounds were excited at the low energy visible band maxima (see Table 1). For compounds **4-6** and Fc-DPP control, fluorescence peak intensity was too low to report.

The fluorescence peak maxima for TPA-control and DPP-control were located at 395 and 612 nm, respectively. For compounds **1-3**, the DPP emission was found to be red-shifted up to 16 nm with about 27-35% quenching suggesting moderate level of excited state interactions (Figure 2c). The degree of quenching followed the order: **3** > **2** > **1**. This was also the case in the measured fluorescence lifetimes determined using time correlated single photon counting technique (TCSPC). A lifetime of 3.98 ns was recorded for DPP-control, while for **1-3**, respective lifetimes of 3.78, 2.48 and 2.31 ns (all monoexponential decays) were obtained. Assuming the quenching is due to electron transfer (*vide infra*), the rate constants for charge separation (k_{CS}) for compounds **1-3** were calculated from the lifetime data and are also listed in Table 1. Although the trends in k_{CS} followed that of the steady-state fluorescence quenching, the magnitude of such values suggest relatively slower charge separation process. Interestingly, introducing ferrocenyl entity on terminal position of

thienyl-DPP caused quantitative quenching in the case of **4-6** suggesting occurrence of efficient excited state events.

Electrochemical studies using cyclic and differential pulse voltammetry (DPV) were subsequently performed. Figures 3a and b show DPVs of the investigated compounds in DCB containing 0.1 M (TBA)ClO₄. The reduction of the dithienyl-DPP entity appeared in the potential range of -0.91 - -1.02 V vs. Ag/AgCl while the TPA oxidation appeared in the range of 1.00 - 1.10 V, and ferrocene oxidation in compounds **4-6** was in the range of 0.73 - 0.76 V vs. Ag/AgCl. Electrochemical reversibility of these electrode processes were confirmed by cyclic voltammetry. Gradual anodic shift of DPP reduction, and cathodic shift of TPA and Fc oxidations upon gradual increase in their number was witnessed. The net result of this anodic and cathodic shifts of reduction and oxidation processes is lowering the electrochemical HOMO-LUMO gap. For example, the HOMO-LUMO gap for **1** was 2.02 V that shrunk to 1.99 V for **3**, while this gap was 1.75 V for **4** that shrunk to 1.62 eV for **6**. This trend agreed well with the earlier discussed absorption and fluorescence spectral trends, where systematic red-shift of peak maxima as a result of lowered HOMO-LUMO gap was witnessed.

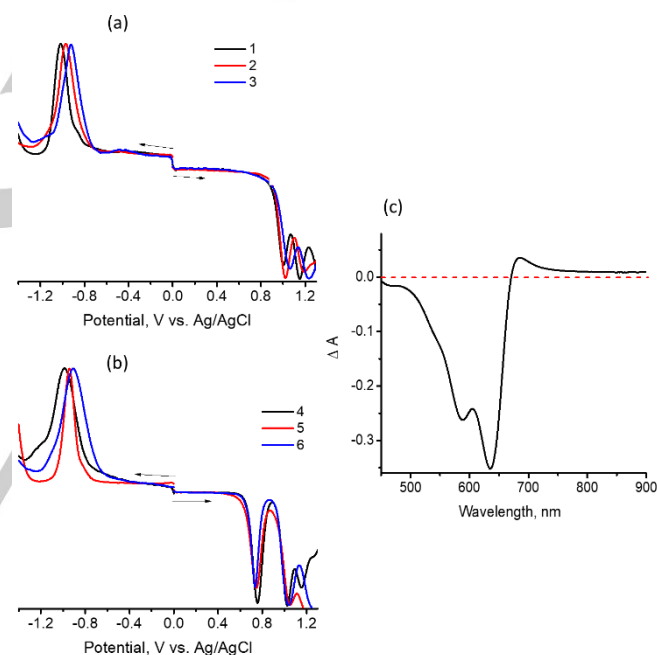


Figure 3. Differential pulse voltammograms (DPVs) of (a) **1-3** and (b) **4-6** in DCB containing 0.1 M (TBA)ClO₄. (c) Spectrum of the charge separated state generated from averaging the differential absorption spectrum of the first oxidized and first reduced species of **4**.

Next, spectroelectrochemical studies were performed to spectrally characterize the oxidized and reduced species. Individual spectral changes during oxidation and reduction processes of the investigated compounds are shown in Figure S16 in SI. To generate the spectrum of the charge separated species, average of the differential absorption spectrum of the first oxidized and first reduced species were utilized, as shown in Figure 3c. This spectral manipulation resulted in two peaks at 606 and 685 nm, and depleted peaks at 470, 588 and 635 nm for the charge separated species. Presence of such spectral features in the transient absorption spectral recordings would provide evidence of excited state charge separation in these donor-acceptor conjugates.

Energy level diagrams were constructed to visualize excited state events in compounds **1-3** (Figure S17) and **4-6** (Figure 4) by using spectral, electrochemical and geometry parameters from energy optimized structures (see Figure S18 in SI for optimized structures), according to Rehm-Weller approach.^[20,21] Formation of $\text{DPP}^{\cdot-}\text{-TPA}^{\cdot+}$ charge separated states upon excitation of bithienyl-DPP entity in compounds **1-3** was thermodynamically feasible. The energy of the charge separated states varied between 1.88 – 1.91 eV revealing their high potential status, however, the earlier discussed steady-state and time-resolved fluorescence studies suggested such excited state charge transfer being inefficient. Interestingly, for compounds **4-6** where total quenching of DPP was observed, as expected, formation of $\text{Fc}^{\cdot+}\text{-DPP}^{\cdot-}\text{-TPA}$ charge separated state was also thermodynamically feasible. Owing to the redox modulation of the donor and acceptor entities, the energy of the charge-separated states followed the order: $\text{Fc-DPP control} > \mathbf{4} > \mathbf{5} > \mathbf{6}$. Consequently, according to Marcus electron transfer theory, one would expect the rate constants for charge separation (k_{CS}) and recombination (k_{CR}) would be different although they are primarily derived from the Fc-DPP part of the conjugates.^[22] Additionally, from the difference between the free energy change of charge separation and recombination processes (Figure 4), it is evident that the charge separation process to belong to the normal region while

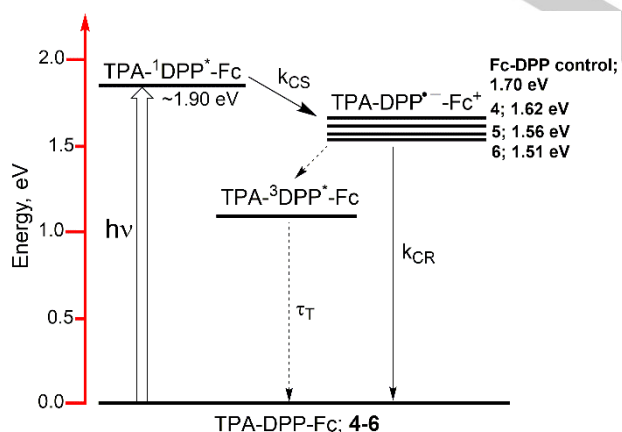


Figure 4. Energy level diagram showing different photochemical events in Fc-DPP-TPA derived star-shaped donor-acceptor conjugates.

the charge recombination to belong to inverted region of Marcus parabola. The CSS could relax directly to the ground state or populate the 3 dithienyl-DPP* state for which an energy of 1.1 eV has been earlier reported.^[23] If the latter path is supposed to occur then one would expect faster charge recombination.

The results summarized above predicted several interesting trends including, (i) efficient quenching in **4-6** compared to that in **1-3**, and (ii) variation in k_{CS} and k_{CR} in case of **4-6** as a result of redox modulation with increasing number of Fc-DPP entities on the central TPA. In order to experimentally demonstrate such trends, femtosecond transient absorption (fs-TA) studies were performed and the results are summarized below.

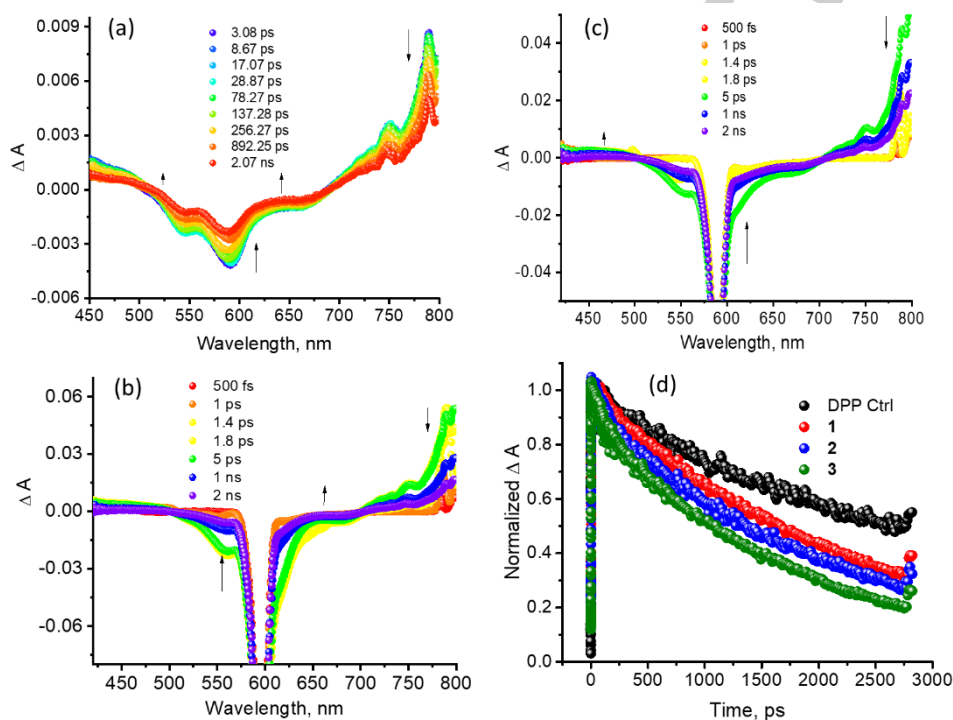


Figure 5. fs-TA spectra at the indicated delay times of (a) DPP-control, (b) **1** and (c) **3** in DCB. The samples were excited at visible peak maxima (595-620 nm). Decay profiles of the singlet peak monitored at 797 nm is shown in figure 5d.

Table 2. Determined k_{CS} and k_{CR} from fs-TA data in DCB for the investigated compounds.

Compound	solvent	$k_{\text{CS}} \times 10^{-10} \text{ s}^{-1}$	$k_{\text{CR}} \times 10^{-8} \text{ s}^{-1}$
Fc-DPP control	DCB	3.85	1.0
4	DCB	4.16	0.43
5	DCB	5.00	0.41
6	DCB	6.67	0.40

Figure 5a shows the fs-TA at the indicated delay times of DPP-control in DCB. The Instantaneously formed $^1\text{DPP}^*$ revealed positive peaks at 750 and 790 nm due to excited state absorption (ESA) and negative peaks at 543, 591 and 653 nm.^[16] The 543 nm peak was solely due to ground state bleach (GSB) while the 591 nm peak had contributions from GSB and stimulated emission (SE). The 653 nm peak was due to SE. The decay of ESA and recovery of the GSB and SE peaks were slow in accordance with longer lifetime of $^1\text{DPP}^*$ -control being 3.98 ns. Fs-TA spectra for **1** and **3** are shown in Figure 5b and c, respectively (see Figure S19a for fs-TA spectra of **2**). Gradual red-shift of ESA in the near-IR region, GSB and SE peaks in the visible region of $^1\text{DPP}^*$ was observed for all three compounds. As predicted for slow CS process, no new peaks within the monitoring time window was apparent. The time profile of the near-IR ESA peak is shown in Figure 5d. In accordance with the

fluorescence lifetime data, the decay followed the trend: DPP control $< 1 < 2 < 3$. Decay time constants of 2257, 2056 and 1520 ps, respectively, for **1**, **2**, and **3** were obtained that largely agreed with the fluorescence lifetime values.

In contrast, the photochemical events in Fc-DPP derived compounds were rapid exhibiting peaks corresponding to the formation of charge separated states. In all of these compounds, the near-IR peak corresponding to $^1\text{DPP}^*$ ESA decayed within few ps with new peaks expected for CSS from earlier discussed spectroelectrochemical studies (Figure 6). For example, in the case of Fc-DPP control, new peaks at 600 and 678 nm and depleted peaks at 572 and 628 nm corresponding to the formation of $\text{Fc}^+\text{-DPP}^-$ CSS was observed (Figure 6a). Similar trends were also observed for **4-6** (Figures 6b and c), however, peaks corresponding to CSS in the visible region were slightly red-shifted (see Figure S19b for fs-TA spectra of **5**). From the growth of the CSS peak at ~ 680 nm, the k_{CS} values were calculated (Table 2) and these values followed the trend: Fc-DPP control $< 4 < 5 < 6$.

The decay profile of the ~ 680 nm peak corresponding to the CSS was monitored to secure information on k_{CR} values. Decay profiles are shown in Figure 6d reveals unusually long-lived CSS. By extrapolation of the decay curves, k_{CR} values were estimated as listed in Table 2. These k_{CR} values were slower by 2-3 orders of magnitude compared to k_{CS} and some of the simpler DPP

expected. It is likely that the recombination path does not rigorously follow the predicted path of direct charge recombination to the ground state but might involve different degrees of electronic coupling in these star-shaped supramolecular systems ultimately prolonging the lifetime of charge-separated states. The current results nicely demonstrate how redox modulation in multimodular donor-acceptor conjugates direct the kinetics of excited state electron transfer events.^[24]

In summary, the newly synthesized star-shaped, multimodular donor-acceptor-donor type conjugates revealed several noteworthy findings. First, the central TPA entity promoted intramolecular interactions both in the ground and excited states involving terminal DPP in the case of **1-3** and Fc-DPP in the case of **4-6** compounds. Electrochemical studies revealed that the reduction involving the DPP entity in these systems is perturbed more than the oxidation potentials located on Fc and TPA entities. Due to moderate level of quenching in **1-3**, establishing charge separated states from fs-TA studies was challenging, however, in the case of **4-6**, this was possible wherein the transient peaks representing CSS agreed well with that predicted from spectroelectrochemical results. The charge recombination process persisted longer than that reported earlier for simple donor-acceptor conjugates involving DPP, suggesting that the electron coupling between the Fc-DPP and TPA entities are likely the cause for this unprecedented phenomenon. Further studies

to fully understand this unusual phenomenon of charge stabilization in star-shaped donor-acceptor-donor multimodular systems are underway in our laboratories.

Acknowledgements

We acknowledge funding from the DST, (DST/TMD/SERI/D05(C)), INSA (SP/YSP/139/2017/2293), SERB CRG/2018/000032 and CSIR 01(2934)/18/EMR-II, New Delhi Government of India, and US-National Science Foundation (2000988 to FD).

Conflict of interest

The authors declare no conflict of interest.

Keywords: bithienyl diketopyrrolopyrrole

• strongly coupled donor-acceptor-donor conjugates • charge stabilization • ultrafast transient spectroscopy

References and Notes

- [1] (a) A. Facchetti, *Chem. Mater.* **2011**, *23*, 733–758; (b) A. Mishra, P. Bäuerle, *Angew. Chemie.* **2012**, *51*, 2020–2067; (c) Y. Chen, X. Wan, G. Long, *Acc. Chem. Res.* **2013**, *46*, 2645–2655; (d) C. Wang, H. Dong, W. Hu, Y. Liu, D. Zhu, *Chem. Rev.* **2012**, *112*, 2208–2267; (e) N. Kobayashi, S. Inagaki, V. N. Nemykin, T. Nonomura, *Angew. Chemie.* **2001**, *40*, 2710–2712; (f) C. Ji, L. Yin, K. Li, L. Wang, X. Jiang, Y. Suna, Y. Li, *RSC Adv.*

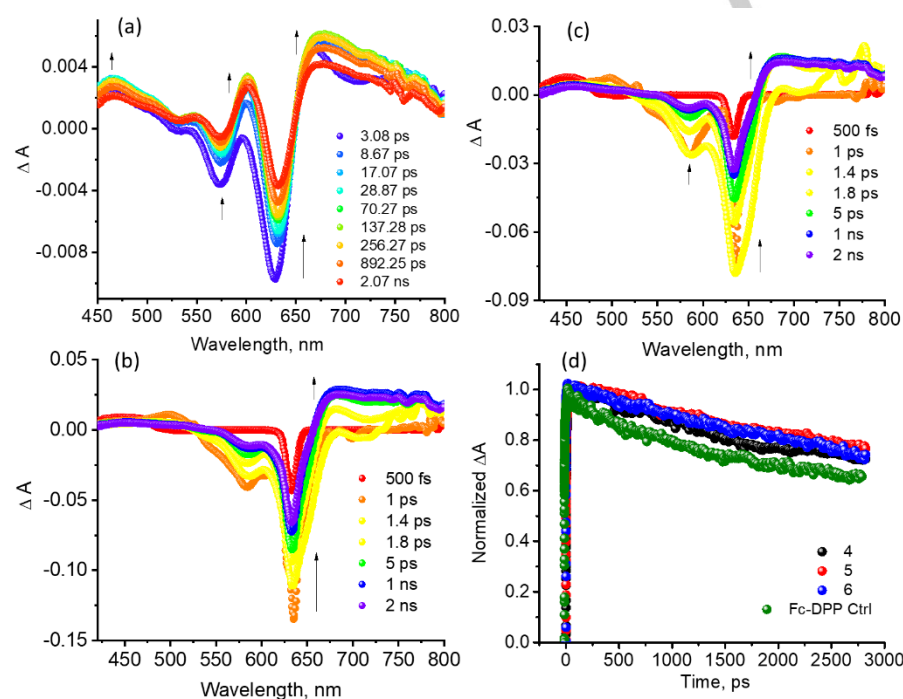


Figure 6. fs-TA spectra at the indicated delay times of (a) Fc-DPP control, (b) **4** and (c) **6**, excited at visible peak maxima (620–635 nm) of a given compound. Time profile of the CSS peak monitored at 680 nm is shown in figure 6d.

derived donor-acceptor systems reported in literature.^[16] This trend could be attributed to the CR process that belongs to the inverted region of Marcus parabola.^[21] Additionally the decay plots also show relatively faster decay for the Fc-DPP control (green trace) compared to the Fc-DPP-TPA derived systems following the trend: Fc-DPP control $> 4 > 5 > 6$. If Marcus free-energy relations were strictly followed, a reverse trend were to be

- 2015, 5, 31606–31614; (g) W. Y. Wong, W. K. Wong, P. R. Raithby, *J. Chem. Soc., Dalton Trans.* **1998**, 0, 2761–2766.
- [2] (a) S. Rochat, T. M. Swager, *ACS Appl. Mater. Interfaces* **2013**, 5, 4488–4502; (b) L. Duan, L. Hou, T.-W. Lee, J. Qiao, D. Zhang, G. Dong, L. Wang, Y. Qiu, *J. Mater. Chem.* **2010**, 20, 6392–6407; (c) L. Zhang, N. S. Colella, B. P. Cherniawski, S. C. B. Mannsfeld, A. L. Briseno, *ACS Appl. Mater. Interfaces* **2014**, 6, 5327–5343; (d) S. Ellinger, K. R. Graham, P. Shi, R. T. Farley, T. T. Steckler, R. N. Brookins, P. Taranekar, J. Mei, L. A. Padilha, T. R. Ensley, H. Hu, S. Webster, D. J. Hagan, E. W. Van Stryland, K. S. Schanze, J. R. Reynolds, *Chem. Mater.* **2011**, 23, 3805–3817.
- [3] (a) N. Armaroli, V. Balzani, *Angew. Chemie.* **2007**, 46, 52–66; (b) P. M. Beaujuge, J. M. J. Frechet, *J. Am. Chem. Soc.* **2011**, 133, 20009–20029. (c) F. D'Souza, O. Ito, *Chem. Soc. Rev.* **2012**, 41, 86. (d) El-Khouly, M. E.; Fukuzumi, S.; D'Souza, F. *ChemPhysChem* **2014**, 15, 30. (e) a) *Organic Nanomaterials* Eds. T. Torres, G. Bottari, Wiley-VCH, Weinheim, 2013. (f) H. Imahori, T. Umeyama, S. Ito, *Acc. Chem. Res.*, **2009**, 42, 1809–1818. (g) D. Gust, T. A. Moore, A. L. Moore, *Faraday Discuss.* **2012**, 155, 9. (h) N. Martin, L. Sanchez, M. A. Herranz, B. Illesca, D. M. Guldi, *Acc. Chem. Res.*, **2007**, 40, 1015–1024, (i) G. Bottari, G. de la Torre, D. M. Guldi, T. Torres, *Chem. Rev.*, **2010**, 110, 6768–6816.
- [4] (a) J. Zyss, I. Ledoux, *Chem. Rev.* **1994**, 94, 77–105; (b) H. M. Kim, B. R. Cho, *J. Mater. Chem.* **2009**, 19, 7402–7409; (c) F. Cherioux, H. Maillotte, P. Audebert, J. Zyss, *Chem. Commun.* **1999**, 0, 2083–2084.
- [5] (a) B. R. Cho, K. H. Son, S. H. Lee, Y. S. Song, Y. K. Lee, S. J. Jeon, J. H. Choi, H. Lee, M. Cho, *J. Am. Chem. Soc.* **2001**, 123, 10039–10045; (b) G. Hennrich, I. Asselberghs, K. Clays, A. Persoons, *J. Org. Chem.* **2004**, 69, 5077–5081; (c) B. L. Rupert, W. J. Mitchell, A. J. Ferguson, M. E. Keose, W. L. Rance, G. Rumbles, D. S. Ginley, S. E. Shaheen, N. Kopidakis, *J. Mater. Chem.* **2009**, 19, 5311–5324; (d) S. Roquet, A. Cravino, P. Leriche, O. Alevaque, P. Frere, J. Roncali, *J. Am. Chem. Soc.* **2006**, 128, 3459–3466; (e) H. Inomata, K. Goushi, T. Masuko, T. Konno, T. Imai, H. Sasabe, J. J. Brown, C. Adachi, *Chem. Mater.* **2004**, 16, 1285–1291.
- [6] (a) M. van, Ham, J. A. J. M. Vekemans, E. E. Havinga, E. W. Meijer, *Mater. Sci. Eng. R-Rep.* **2001**, 32, 1–40; (b) Y. Zhang, J. Zou, H.-L. Yip, K.-S. Chen, D. F. Zeigler, Y. Sun, A. K.-Y. Jen, *Chem. Mater.* **2011**, 23, 2289–2291. (c) C. B. KC, F. D'Souza, *Coord. Chem. Rev.* **2016**, 322, 104–141. (d) *Multiporphyrin Array: Fundamentals and Applications*, (Ed. D. Kim), Pan Stanford Publishing: Singapore, 2012. (e) R. Canton-Vitoria, H. B. Gobeze, V. M. Blas-Ferrando, J. Ortiz, Y. Jang, F. Fernandez-Lazaro, A. Sastre-Santos, Y. Nakanishi, H. Shinohara, F. D'Souza, N. Tagmatarchis, *Angew. Chem. Int. Ed.* **2019**, 58, 5712–5717.
- [7] (a) Y. Patil, T. Jadhav, B. Dhokale, R. Misra, *Eur. J. Org. Chem.* **2016**, 733–738; (b) Y. Patil, R. Misra, M. L. Keshtov, G. D. Sharma, *J. Mater. Chem. A*, **2017**, 5, 3311–3319. (b) Y. Patil, R. Misra, M. L. Keshtov, G. D. Sharma, *J. Phys. Chem. C* **2016**, 120, 6324–6335; (d) Y. Patil, R. Misra, F. C. Chen, M. L. Keshtov, G. D. Sharma, *RSC Adv.* **2016**, 6, 99685–99694.
- [8] (a) J. Chen, Y. Cao, *Acc. Chem. Res.* **2009**, 42, 1709–1718; (b) Y. J. Cheng, S. H. Yang, C. S. Hsu, *Chem. Rev.* **2009**, 109, 5868–5923.
- [9] (a) Y. Lin, L. Ma, Y. Li, Y. Liu, D. Zhu, X. Zhan, *Adv. Energy Mater.* **2013**, 3, 1166–1170; (b) Y. Lin, Y. Li, X. Zhan, *Adv. Energy Mater.* **2013**, 3, 724–728; (c) Y. Qiao, Y. Guo, C. Yu, F. Zhang, W. Xu, Y. Liu, D. Zhu, *J. Am. Chem. Soc.* **2012**, 134, 4084–4087.
- [10] (a) K. Schmidt, C. J. Tassone, J. R. Niskala, A. T. Yiu, O. P. Lee, T. M. Weiss, M. F. Toney, *Adv. Mater.* **2014**, 26, 300–305; (b) B. Lim, J. S. Yeo, D. Khim, D. Y. Kim, *Macromol. Rapid Commun.* **2011**, 32, 1551–1556; (c) M. Grzybowski, D. T. Gryko, *Adv. Opt. Mater.* **2015**, 3, 280–320; (d) J. S. Ha, K. H. Kim, D. H. Choi, *J. Am. Chem. Soc.* **2011**, 133, 10364–10367; (e) R. Lenz, O. Wallquist, *Surf. Coat. Int. Part B* **2002**, 85, 19–26.
- [11] (a) L. Dou, J. You, J. Yang, C. C. Chen, Y. He, S. Murase, T. Moriarty, K. Emery, G. Li, Y. Yang, *Nat. Photonics* **2012**, 6, 180–185; (b) W. Li, A. Furlan, K. H. Hendriks, M. M. Wienk, R. A. J. Janssen, *J. Am. Chem. Soc.* **2013**, 135, 5529–5532; (c) K. H. Hendriks, G. H. L. Heintges, V. S. Gevaerts, M. M. Wienk, R. A. Janssen, *Angew. Chemie.* **2013**, 52, 8341–8344.
- [12] (a) Y. Patil, R. Misra, *Chem. Asian J.* **2018**, 13, 220–229; (b) M. Grzybowski, D. T. Gryko, *Adv. Optical Mater.* **2015**, 3, 280–320; (c) Y. Patil, R. Misra, *Chem. Rec.* **2018**, 9, 1350–1364.
- [13] (a) Y. Patil, R. Misra, *J. Mater. Chem. C*, **2019**, 7, 13020–13031. (b) Y. Patil, R. Misra, *Chem. Rec.* **2020**, doi:10.1002/tcr.201900061.
- [14] (a) L. J. Huo, J. H. Hou, H. Y. Chen, S. Q. Zhang, Y. Jiang, T. L. Chen, Y. Yang, *Macromolecules* **2009**, 42, 6564–6571; (b) B. Walker, A. B. Tomayo, X. D. Dang, P. Zalar, J. H. Seo, A. Garcia, M. Tantiwivat, T. Q. Nguyen, *Adv. Funct. Mater.* **2009**, 19, 3063–3069; (c) Y. Z. Lin, P. Cheng, Y. F. Li, X. W. Zhan, *Chem. Commun.* **2012**, 48, 4773–4775; (d) D. Sahu, C. H. Tsai, H. Y. Wei, K. C. Ho, F. C. Chang, C. W. Chu, *J. Mater. Chem.* **2012**, 22, 7945–7953.
- [15] (a) N. Krauß, M. Kielmann, J. Ma, H. Butenschön, *Eur. J. Org. Chem.* **2015**, 2622–2631; (b) S. I. Kato, M. Kivala, W. B. Schweizer, C. Boudon, J. P. Gisselbrecht, F. Diederich, *Chem. Eur. J.* **2009**, 15, 8687–8691. (c) R. Kaur, F. Possanza, F. Limosani, S. Bouroth, R. Zanon, T. Clark, G. Arrigoni, P. Tagliatesta, D. M. Guldi, *J. Am. Chem. Soc.* **2020**, 142, 7898–7911. (d) S. Kaur, M. Kaur, P. Kur, K. Clays, K. Singh, *Coord. Chem. Rev.* **2017**, 343, 185–219. (e) G. N. Lim, E. Maligaspe, M. E. Zandler, F. D'Souza, *Chem. Eur. J.* **2014**, 20, 17089–17099. (f) M. A. Collini, M. B. Thomas, V. Bandi, P. A. Karr, F. D'Souza, *Chem. Eur. J.* **2017**, 23, 4450–4461. (g) C. Chakraborty, B. Chanchal, K. Manas, U. Rana, S. Malik, *Chem. Commun.* **2015**, 51, 13123–13126. (h) T. Michinobu, H. Kumazawa, K. Noguchi, K. Shigehara, *Macromolecules*, **2009**, 42, 5903–5905. (i) M. Kondo, M. Uchikawa, K. Namiki, W.-W. Zhang, S. Kume, E. Nishihori, H. Suwa, S. Aoyagi, M. Sakata, M. Murata, Y. Kobayashi, H. Nishihara, *J. Am. Chem. Soc.* **2009**, 131, 12112–12124. (j) C. A. Wijesinghe, M. E. El-Khouly, M. E. Zandler, S. Fukuzumi, F. D'Souza, *Chem. Eur. J.* **2013**, 19, 9629–9638. (k) H. Imahori, Y. Sekiguchi, Y. Kashiwagi, T. Sato, Y. Araki, O. Ito, H. Yamada, S. Fukuzumi, *Chem. Eur. J.* **2004**, 10, 3184–3196.
- [16] (a) H. G. Ryu, M. F. Mayther, J. Tamayo, C. Azarias, D. M. Espinoza, M. Banasiewicz, Y. M. Poronik, A. Jezewski, J. Clark, J. B. Derr, K. H. Ahn, D. T. Gryko, D. Jacquemin, V. I. Vullev, *J. Phys. Chem.* **2018**, 122, 12424–12434. (b) D. Ley, C. X. Guzman, K. H. Adofsson, A. M. Scott, A. B. Braunschweig, *J. Am. Chem. Soc.* **2014**, 136, 7809–7812. (c) Q. A. Alsulami, S. M. Aly, S. Goswami, E. Alarousu, A. Usman, K. S. Schanze, O. F. Mohammed, *J. Phys. Chem. C* **2015**, 119, 15910–15925. (d) W. Kim, Y. Sung, M. Grzybowski, D. To. Gryko, D. Kim, *J. Phys. Chem. Lett.* **2016**, 7, 3060–3066. (e) A. Purc, E. M. Espinoza, R. Nazir, J. J. Romero, K. Skonieczny, A. Jezewski, J. M. Larssen, D. T. Bryko, V. I. Vullev, *J. Am. Chem. Soc.* **2016**, 138, 12826–12832.
- [17] (a) Z. Lu, C. Li, T. Fang, G. Li, Z. Bo, *J. Mater. Chem. A* **2013**, 1, 7657–7665; (b) Y. Jiang, D. Yu, L. Lu, C. Zhan, D. Wu, W. You, Z. Xie, S. Xiao, *J. Mater. Chem. A* **2013**, 1, 8270–8279; (c) S. Zhang, B. Jiang, C. Zhan, J. Huang, X. Zhang, H. Jia, A. Tang, L. Chen, J. Yao, *Chem. Asian J.* **2013**, 8, 2407–2416; (d) P. Leriche, F. Piron, E. Ripaud, P. Frere, M. Allain, J. Roncali, *Tetrahedron Lett.* **2009**, 50, 5673–5676.
- [18] (a) P. Dutta, W. Yang, S. H. Eom, S. H. Lee, *Org. Electron.* **2012**, 13, 273–282; (b) J. Zhang, Y. Yang, C. He, D. Deng, Z. B. Li, Y. F. Li, *J. Phys. D: Appl. Phys.* **2011**, 44, 475101–475105; (c) Y. Yang, J. Zhang, Y. Zhou, G. J. Zhao, C. He, Y. F. Li, M. Andersson, O. Inganäs, F. L. Zhang, *J. Phys. Chem. C* **2010**, 114, 3701–3706; (d) P. Zhou, D. Dang, M. Xiao, Q. Wang, J. Zhang, H. Tan, Y. Pei, R. Yang, W. Zhu, *J. Mater. Chem. A* **2015**, 3, 10883–10889.
- [19] (a) S. Roquet, R. de Bettignies, P. Leriche, A. Cravino, J. Roncali, *J. Mater. Chem.* **2006**, 16, 3040–3045; (b) S. Shoaee, S. Subramaniyan, H. Xin, C. Keiderling, P. S. Tuladhar, F. Jamieson, S. A. Jenekhe, J. R. Durrant, *Adv. Funct. Mater.* **2013**, 23, 3286–3298. (c) M. Supur, Y. Kawashima, K. Mase, K. Ohbubo, T. Hasobe, S. Fukuzumi, *J. Phys. Chem. C* **2015**, 119, 13488–13495. (d) C. Siegers, B. Olah, U. Wuerfel, J. Hohl-Ebinger, A. Hinsch, R. Haag, *Solar Energy Materials & Solar Cells*, **2009**, 93, 552–563.
- [20] D. Rehm, A. Weller, *Isr. J. Chem.*, **1970**, 8, 259.
- [21] Gibbs free-energy change associated for excited state charge separation (CS) and dark charge recombination (CR) were estimated according to equations 1–3

COMMUNICATION

$$-\Delta G_{CR} = E_{ox} - E_{red} + \Delta G_S \quad (i)$$

$$-\Delta G_{CS} = \Delta E_{00} - (-\Delta G_{CR}) \quad (ii)$$

where ΔE_{00} corresponds to the energy of ${}^1\text{DPP}^*$ (= 1.90 eV). The term ΔG_S refers to electrostatic energy calculated according to dielectric continuum model (see equation iii). The E_{ox} and E_{red} represent the oxidation potential of the electron donor (Fc) and the first reduction potential of the electron acceptor (DPP), respectively.

$$\Delta G_S = e^2/4 \pi \epsilon_0 \left[-1/R_{CC} \epsilon_R \right] \quad (iii)$$

The symbols ϵ_0 and ϵ_R represent vacuum permittivity and dielectric constant of DCB used for photochemical and electrochemical studies (= 9.93). R_{CC} are the center-to-center distance between donor and acceptor entities from the computed structures in Figure S18.

[22] a) R. A. Marcus, N. Sutin, *Biochim. Biophys. Acta* **1985**, 811, 265.

b) R. A. Marcus, *Angew. Chem. Int. Ed. Engl.* **1993**, 32, 1111.

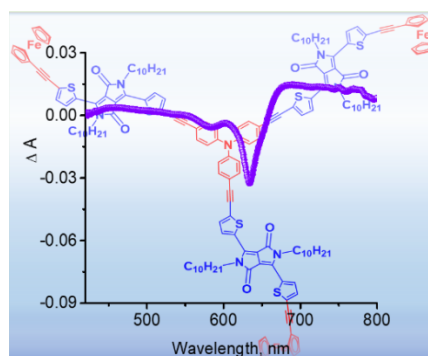
[23] B. P. Karsten, R. K. M. Bouwer, J. C. Hummelen, R. M. Williams, R. A. J. Janssen, *Photochem. Photobiol. Sci.*, **2010**, 9, 1055-1065.

[24] N. Zarrabi, S. Seetharaman, S. Chaudhuri, N. Holzer, V. S. Batista, A. van der Est, F. D'Souza, P. K. Poddutoori, *J. Am. Chem. Soc.* **2020**, 142, 10008-10024.

Entry for the Table of Contents

COMMUNICATION

The significance of multiple donor-acceptor entities appended on a central donor in a star-shaped molecular system for improved light harvesting is reported. The donor-acceptor-donor conjugates comprised of up to three entities of ferrocenyl (Fc)-diketopyrrolopyrrole (DPP) onto a central triphenylamine (TPA). Due to strong electron coupling between the entities, long-lived charge separation was possible to achieve.



C. Popli, Y. Jang, Y. Patil, R. Misra* and F. D'Souza*

Page No. – Page No.

Formation of Highly Efficient, Long-Lived Charge Separated States in Star-Shaped Ferrocene-Diketopyrrolopyrrole-Triphenylamine Donor-Acceptor-Donor Conjugates